immuno

MDPI

Article

Anti-Inflammatory Efficacy of Resveratrol-Enriched Rice Callus Extract on Lipopolysaccharide-Stimulated RAW264.7 Macrophages

Chaiwat Monmai, Jin-Suk Kim and So-Hyeon Baek *

Department of Agricultural Life Science, Sunchon National University, Suncheon 59722, Republic of Korea; bbuayy@gmail.com (C.M.); kimjs6911@naver.com (J.-S.K.)
* Correspondence: baeksh@scnu.ac.kr; Tel.: +82-61-750-3217

Abstract: Resveratrol and its derivative piceid exhibit a wide spectrum of health-promoting bioactivities. A resveratrol-enriched variety of Dongjin rice (DJ526) has been developed by transfection of a resveratrol biosynthesis gene, and increased resveratrol content has been confirmed in seeds following germination. In the current study, these resveratrol-enriched seeds were induced to produce callus, and callus extracts were evaluated for in vitro anti-inflammatory activity. Callus cultures contained greater amounts of resveratrol and piceid than DJ526 seeds, and treatment with DJ526 callus extract significantly reduced the lipopolysaccharide (LPS)-induced production of proinflammatory mediators nitric oxide and prostaglandin E2 by RAW264.7 macrophages. The inflammation-related nuclear factor kappa B and mitogen-activated protein kinase pathways were also inhibited in DJ526 callus extract-treated RAW264.7 cells, resulting in downregulation of proinflammatory factor genes *COX-2*, *iNOS*, *IL-1β*, *IL-6*, and *TNF-α*. Expression of the LPS-binding toll-like receptor-4 was also markedly reduced in DJ526 callus extract-treated cells compared to DJ callus extract-treated cells. These findings demonstrate increased resveratrol and piceid content by callus culture of DJ526 rice seeds and the potent anti-inflammatory activity of resveratrol-enriched callus extract.

Keywords: resveratrol; piceid; LPS; PGE_2 production; NO production; proinflammatory cytokines

Citation: Monmai, C.; Kim, J.-S.; Baek, S.-H. Anti-Inflammatory Efficacy of Resveratrol-Enriched Rice Callus Extract on Lipopolysaccharide-Stimulated RAW264.7 Macrophages. *Immuno* **2024**, *4*, 131–146. https://doi.org/10.3390/immuno4020009

Academic Editors: Bashar Saad and Badiaa Lyoussi

Received: 11 January 2024
Revised: 26 March 2024
Accepted: 1 April 2024
Published: 3 April 2024

1. Introduction

Inflammation is a protective immune response initiated by a host cell against harmful stimuli such as pathogens, the contents of damaged cells, and various chemical and physical irritants [1]. In most tissues, inflammation is initiated by resident macrophages, which recognize various pathogen- and damage-associated molecular patterns, transition to an activated phenotype, and subsequently secrete proinflammatory factors that drive subsequent inflammatory pathways [2]. These responses are mediated by surface receptor activation and downstream activation of the nuclear factor kappa B (NF-κB) and mitogen-activated protein kinase (MAPK) pathways [3]. Bacterial lipopolysaccharide (LPS) is a potent activator of macrophages [4,5] and is widely used for experimental activation of inflammatory pathways [6–9]. Lipopolysaccharide binds to toll-like receptor-4 (TLR-4), leading to the activation of NF-κB and MAPK [3,10], which in turn promotes the synthesis and secretion of proinflammatory mediators (cytokines, chemokines, and enzymes) such as prostaglandin E2 (PGE_2), nitric oxide (NO), interleukin (IL)-1β, IL-6, tumor necrosis factor (TNF)-α, and cyclooxygenase-2 (COX-2) [3,11,12].

Resveratrol is a natural polyphenol found in grapes [13], various berries [14], peanuts [15], and plums [16]. Resveratrol and its derivative piceid have been demonstrated to promote multiple processes beneficial to health, including antioxidant [17,18], antifungal, antibacterial [19], anticancer [20,21], and anti-inflammatory activities [22–24]. Moreover, these effects contribute to the observed efficacy of these compounds in models

of Alzheimer's disease [25,26] and Parkinson's disease [27]. Resveratrol has been demonstrated to be in vitro and in vivo anti-inflammatory in several studies. Zhong et al. [28] reported that treatments with resveratrol significantly decreased the production of NO and PGE_2 in LPS-stimulated BV-2 cells. In addition, the expression of inflammatory-associated cytokines (iNOS, IL-1β, COX-2, and TNF-α) was also suppressed in LPS-stimulated BV-2 cells when supplemented with resveratrol [28]. In LPS-stimulated monocytes, treatment with resveratrol led to inhibition of LPS-induced inflammatory mediators such as TNF-α, IL-8, and monocyte chemoattractant protein-1 (MCP-1) [29]. Moreover, an in vivo mouse model exhibited that the long-term treatment of resveratrol in aged mice is able to decrease acute inflammatory stimuli by LPS [30]. In 2013, the resveratrol biosynthesis gene *Arachis hypogaea* stilbene synthase (STS) from the pods of the peanut cultivar Palkwang was introduced into Dongjin rice (DJ) to create resveratrol-enriched rice [31]. The *AhSTS1* cDNA was inserted between the BamHI and SacI sites under the control of the *Ubi1* promoter of the binary vector pSB22. The seed extract from this genetically modified rice (DJ526) was subsequently demonstrated to exert potent and dose-dependent anti-inflammatory activities in LPS-stimulated RAW264.7 macrophages [32]. In addition, increasing the resveratrol content in rice seed via germination enhanced anti-inflammatory activities compared to nongerminated DJ526 rice seed [32]. Cho and Lim [33] reported that the change in phenylalanine ammonia-lyase and cell wall peroxidase during the gemination of brown rice led to an increase in phenolic acid composition. The increase in phenolic acid content resulted in an enhancement in the antioxidant activity of brown rice. Interestingly, the antioxidant activity of phenolic acid in the shoot fraction was significantly higher than the remaining kernel fraction. From this information, we hypothesized that the resveratrol content would increase in DJ526 rice callus in comparison to the DJ526 rice seed (both germinated and nongerminated seeds). However, the anti-inflammatory activity of resveratrol from the DJ526 rice callus extract needs to be investigated. The increase in resveratrol content in DJ526 rice callus must remain an inflammatory defense activity as well. The resveratrol content of rice seeds may vary annually depending on the growing area or growing environment (light conditions, temperature, rainfall, etc.). Therefore, we have developed the DJ526 rice callus for plant factories to develop a biomaterial with a stable resveratrol content. The current study aimed to further enhance the resveratrol content of DJ526 rice seed by callus induction and evaluate the anti-inflammatory activity of callus extracts on LPS-stimulated RAW264.7 cells.

2. Materials and Methods

2.1. Callus Culture

Wild-type DJ and DJ526 calluses were generated from the corresponding rice seeds according to the method of Khan et al. [34]. Briefly, seeds were sterilized with 70% (v/v) ethanol followed by 2% sodium hypochlorite, washed several times with sterilized distilled water, and induced by inoculation in 2N6 medium at 25 °C for 3 weeks under darkness. Calluses were then cultured in 2MS-NO_3-free liquid medium for 10 days before collection.

2.2. Extraction of Resveratrol-Enrich Compound from Rice Callus

Dried calluses were ground, and a resveratrol-enriched extract was prepared as previously described [32,35]. Briefly, callus samples were incubated in 80% methanol, filtered through 5 µm filter paper, concentrated by rotary evaporation, and lyophilized using a freeze-dry system. The lysophilized samples were dissolved in dimethyl sulfoxide (DMSO) at 10, 25, 50, and 100 mg/mL for experiments.

2.3. Quantification of Piceid and Resveratrol Content Using High-Performance Liquid Chromatography (HPLC) Analysis

Piceid and resveratrol contents in rice callus extracts were determined according to a previously described method [32,36]. Briefly, sample powder was mixed with 80% methanol and sonicated at room temperature for 30 min. The mixture was then centrifuged

at 10,000× *g* and 4 °C for 5 min, and the supernatant was collected, passed through a 0.2 μm filter, and analyzed for piceid and resveratrol content using a Waters e2695 HPLC system (Waters, Milford, MA, USA). Contents were quantified by comparison to a standard curve (Figure S1) generated from known concentrations using Empower software (Empower® 3; Waters).

2.4. RAW264.7 Cell Culture

Macrophages of the RAW264.7 line were acquired from the Korean Cell Line Bank (Seoul, Republic of Korea) and maintained at 37 °C in RPMI-1640 medium (Gibco™) supplemented with phenol red, 10% fetal bovine serum (FBS; Gibco™, Thermo Fisher Scientific, Inc., Waltham, MA, USA), and penicillin/streptomycin (1%; Hyclone Laboratories, Logan, UT, USA) under a 5% CO_2 atmosphere. For treatment, this medium was replaced with RPMI-1640 medium (Gibco™) without phenol red and supplemented with 1% FBS and 1% penicillin/streptomycin.

2.5. Cell Viability and Nitric Oxide Production Analysis

Cells were counted using a hemacytometer and seeded in 96-well plates at 10^5 cells/well, then cultured at 37 °C under a 5% CO_2 atmosphere for 24 h prior to treatment. Extracts were prepared at the indicated concentrations (10, 25, 50, and 100 μg/mL) in the treatment medium and applied to the indicated wells. Aspirin (Sigma-Aldrich, St. Louis, MO, USA) was prepared in treatment medium at 200 μg/mL and applied as the positive control [37,38]. After the indicated treatment for 1 h, the cells were stimulated with LPS at the final concentration of 1 μg/mL (excluding the nontreatment group, which received the same volume of treatment medium). The plate was incubated at 37 °C under a 5% CO_2 atmosphere for 24 h. The culture medium was collected, and nitric oxide (NO) production was measured using the Griess reagent (Sigma-Aldrich), which was prepared in the deionized water at a concentration of 40 mg/mL (working solution). Briefly, the culture medium was mixed with Griess reagent working solution at 1:1 (*v*/*v*) in 96-well plates, and the mixtures were incubated at room temperature for 15 min in the dark. Absorbance at 540 nm was measured, and NO production was quantified using a standard curve for sodium nitrite solution (Figure S2).

Viable cells were then counted by adding 110 μL of the EZ-Cytox Cell Viability Assay Kit working solution (10-fold dilution in 1× PBS; DoGenBio, Seoul, Republic of Korea) to each well. After 4 h of incubation at 37 °C, 100 μL of the solution was transferred to new 96-well plates, and absorbance was measured at 450 nm. Cell viability was calculated by comparing the absorbance value of each treatment group to that of parallel control cultures incubated in treatment medium without extract.

2.6. RNA Isolation, RNA Quantification, and cDNA Synthesis

Cells were seeded as described in 24-well plates at 500,000/well, incubated for 24 h in maintenance medium, and then incubated in treatment medium with the indicated concentration of extract for 1 h prior to stimulation with 1 μg/mL LPS (or vehicle as a control). After 6 h of stimulation, cells were washed twice with 1× PBS and then treated with TriZol reagent™ (Invitrogen, Waltham, MA, USA) at 500 μL/well for RNA extraction. Chloroform (200 μL) was added to each tube. The tubes were centrifuged at 13,000 rpm at 4 °C for 10 min. The upper phrase of the solution was collected. Total RNA was precipitated with 100% isopropanol at 4 °C for 30 min, and the pellet was washed three times with ice-cold 70% ethanol. The RNA pellet was then dissolved in nuclease-free water and stored at −80 °C until analysis. Total RNA was quantified using a SpectraMax® ABS Plus Microplate Reader (Molecular Devices, San Jose, CA, USA) by measuring the 260 nm absorbance, and quality was checked by measuring the 260 nm to 280 nm (A260:A280) absorbance ratio and the A260:A230 ratio. Only samples with ratios of 1.800–2.000 for A260:A280 and A260:A230 were processed further (Table 1). First-strand cDNA was synthesized using 1000 ng of total RNA and a Power cDNA Synthesis Kit (Intron Biotechnology, Seongnam-si, Republic of

Korea). The cDNA was prepared at 5 ng/μL in nuclease-free water for measurement of inflammation-related mRNA expression levels by real-time quantitative polymerase chain reaction (RT-qPCR).

Table 1. The quantity and quality of extracted RNA from each treatment.

Treatment	Concentration	A260:A280	A260:A230	RNA Concentration (ng/μL)	CV *
Nontreatment	–	1.888	1.908	394.05 ± 9.55	2.42
DMSO	0.1%	1.966	1.877	547.81 ± 8.23	1.50
DJ	10 μg/mL	1.927	1.839	453.12 ± 11.64	2.57
DJ	25 μg/mL	1.997	1.955	521.39 ± 10.57	2.03
DJ	50 μg/mL	1.980	1.925	537.57 ± 12.12	2.26
DJ	100 μg/mL	1.912	1.990	1033.92 ± 44.85	4.34
DJ526	10 μg/mL	1.948	1.899	497.55 ± 11.60	2.33
DJ526	25 μg/mL	1.927	1.813	450.40 ± 12.55	2.79
DJ526	50 μg/mL	1.882	1.956	551.36 ± 19.13	3.47
DJ526	100 μg/mL	1.876	1.893	441.44 ± 14.03	3.18
Aspirin	200 μg/mL	1.992	1.930	548.85 ± 13.80	2.51

* The coefficient of variation (CV) is the ratio of the standard deviation to the mean. The lower the value of the coefficient of variation, the more precise the estimate.

2.7. Measurement of mRNA from Inflammatory Genes by RT-qPCR

The mRNA levels of proinflammatory mediators *COX-2* and *iNOS*, cytokines *IL-1β*, *IL-6*, and *TNF-α*, and the LPS receptor toll-like receptor-4 (*TLR-4*) were measured using RealMOD™ Green W^2 2× qPCR Mix (Intron Biotechnology, Seongnam-si, Republic of Korea) and a CFX Connect Real-Time PCR System (Bio-Rad, Hercules, CA, USA). Each 20-μL PCR reaction mixture consisted of 5 ng cDNA template and 0.375 M of each primer (Table 2). The thermocycle conditions for PCR are presented in Table 3. *β-actin* was used as the reference gene. Expression levels were calculated as fold-changes relative to parallel control groups treated with treatment medium alone using CFX Maestro software (Bio-Rad CFX Maestro 1.1).

Table 2. The primer sets used for RT-qPCR.

Gene	Nucleotide Sequence (5′—3′)	Accession Number	Target Size (bp)
COX-2	Forward primer: 1409-AGAAGGAAATGGCTGCAGAA-1428 Reverse primer: 1602-GCTCGGCTTCCAGTATTGAG-1583	NM_011198.5	194
iNOS	Forward primer: 185-TTCCAGAATCCCTGGACAAG-204 Reverse primer: 364-TGGTCAAACTCTTGGGGTTC-345	BC062378.1	180
IL-1β	Forward primer: 531-GGGCCTCAAAGGAAAGAATC-550 Reverse primer: 713-TACCAGTTGGGGAACTCTGC-694	NM_008361.4	183
IL-6	Forward primer: 33-AGTTGCCTTCTTGGGACTGA-52 Reverse primer: 223-CAGAATTGCCATTGCACAAC-204	NM_031168.2	191
TNF-α	Forward primer: 1-ATGAGCACAGAAAGCATGATC-21 Reverse primer: 276-TACAGGCTTGTCACTCGAATT-256	D84199.2	276
TLR-4	Forward primer: 2281-CGCTCTGGCATCATCTTCAT-2300 Reverse primer: 2498-GTTGCCGTTTCTTGTTCTTCC-2478	NM_021297.3	218
β-actin	Forward primer: 605-CCACAGCTGAGAGGGAAATC-624 Reverse primer: 797-AAGGAAGGCTGGAAAAGAGC-778	NM_007393.5	193

Based on the nucleotide position of coding sequences.

Table 3. PCR conditions for estimating mRNA expression levels.

Process	Temperature	Time	Cycle
Predenaturation	95 °C	10 min	1 cycle
Denaturation	95 °C	20 s	40 cycles
Annealing	60 °C	20 s	
Extension	72 °C	30 s	
Final extension	72 °C	5 min	1 cycle

2.8. Prostaglandin E2 (PGE_2) Production

The culture medium was collected following the indicated treatment and centrifuged at 3000 rpm for 10 min at room temperature. The PGE_2 concentration in the supernatant was measured using an enzyme-linked immunosorbent assay kit (ADI900-001; Enzo Life Sciences, Farmingdale, NY, USA), and PGE_2 production was calculated using a standard curve provided with the kit (Figure S3).

2.9. Western Blot Analysis

Protein was extracted from each treated culture using a radioimmunoprecipitation assay (RIPA) buffer (Geneall Biotechnology, Seoul, Republic of Korea) supplemented with 1× Protease Inhibitor Cocktail Kit 5 (Bio-Medical Science Co., Ltd., Seoul, Republic of Korea). Lysate samples were centrifuged at 13,000 rpm and 4 °C for 30 min, and the total protein concentration in the supernatant was quantified using a Bradford reagent (Sigma-Aldrich). Proteins (30 µg per treatment) were separated on 10% polyacrylamide gels and transferred onto nitrocellulose membranes (Immobilon®-P Transfer Membrane; Merck Millipore, Burlington, MA, USA). Membranes were stained with Ponceau solution for 5 min at room temperature, washed several times with tris-buffered saline containing 0.1% tween® 20 detergent (TBST) until the TBST no longer changed the band color, and blocked by incubation in TBST with 5% (w/v) skim milk at room temperature for 2 h. Membranes were then incubated in a blocking solution with antibodies targeting p-ERK 1/2 (1:2000; Cell Signaling Technology, Danvers, MA, USA), p-p38 MAPK (1:2000; Cell Signaling Technology), p-NF-κB p65 (1:2000; Cell Signaling Technology), ERK 1/2 (1:1000; Santa Cruz Biotechnology, Dallas, TX, USA), p38 MAPK (1:1000; Santa Cruz Biotechnology), NF-κB p65 (1:1000; Santa Cruz Biotechnology), and glyceraldehyde-3-phosphate dehydrogenase (GADPH; 1:5000; Santa Cruz Biotechnology) at 4 °C overnight. Blotted membranes were washed in TBST with agitation at room temperature and then incubated in blocking solution containing secondary antibody [goat antirabbit IgG (H + L)-horseradish peroxidase (1:5000; GenDEPOT, Barker, TX, USA) or m-IgG® BP-horseradish peroxidase (1:5000; Santa Cruz Biotechnology)] at room temperature for 2 h. After being washed with TBST, membranes were incubated with Clarity™ Western ECL Substrate (Bio-Rad) at room temperature for 10 min, and signals were recorded using ChemiDoc (Bio-Rad). Densitometric analyses were conducted using Image Lab software (version 6.0.0; Bio-Rad).

2.10. Statistical Analysis

All data are presented as the mean ± standard deviation. Treatment group means were compared by one-way analysis of variance followed by post hoc Duncan's multiple range tests. A $p < 0.05$ was considered significant for all tests, and all calculations were performed using Statistix 8.1 (Statistix, Tallahassee, FL, USA).

3. Results

3.1. Piceid and Resveratrol Contents in Rice Callus Extracts

The piceid and resveratrol contents in the extracts of DJ and DJ526 callus extracts were measured by HPLC (Figure S1). The peak retention time for piceid was 16.688 min, while that of resveratrol was 27.182 min. Neither peak was detected in extract samples from DJ

callus (Figure 1). In DJ526 extract, the mean (±SD) piceid content was 85.43 ± 3.44 μg/g dry weight, and that of resveratrol was 3.94 ± 0.02 μg/g dry weight. Thus, substantial amounts of these compounds remain in DJ526 rice callus after seed induction.

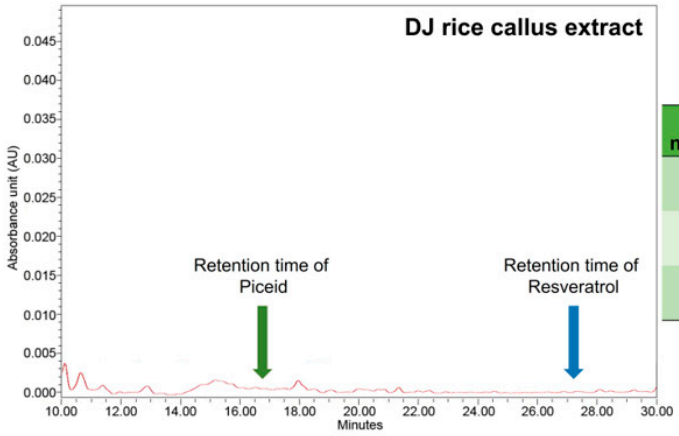

Vail number	Peak name	Retention time (min)	Area	Height	Amount (μg/g dry weight)
1	Piceid	16.688	–	–	–
	Resveratrol	27.182	–	–	–
2	Piceid	16.688	–	–	–
	Resveratrol	27.182	–	–	–
3	Piceid	16.688	–	–	–
	Resveratrol	27.182	–	–	–

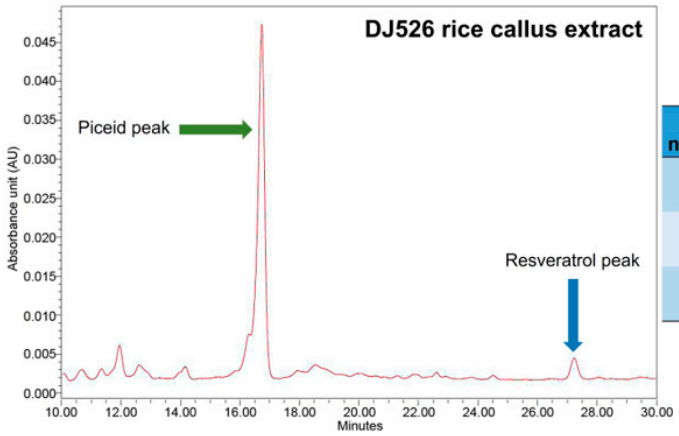

Vail number	Peak name	Retention time (min)	Area	Height	Amount (μg/g dry weight)
1	Piceid	16.774	799314	44615	88.43
	Resveratrol	27.274	43870	2754	3.96
2	Piceid	16.688	778898	44183	86.18
	Resveratrol	27.311	43764	2701	3.95
3	Piceid	16.730	737981	45030	81.67
	Resveratrol	27.239	43446	2682	3.92

Figure 1. Piceid and resveratrol enrichment in DJ526 rice callus extract as measured by high-performance liquid chromatography (HPLC). Sample chromatograms show that piceid and resveratrol are undetectable in DJ rice callus extract (**upper left panel**) but are abundant in DJ526 rice callus extract (**lower left panel**).

3.2. Effects of Resveratrol-Enriched Rice Callus Extract on the Viability of LPS-Stimulated RAW264.7 Cells

The potential cytotoxic effects of rice callus extracts on LPS-stimulated RAW264.7 cells were examined at extract concentrations ranging from 10 to 100 μg/mL (Figure 2). Treatment with LPS alone modestly but significantly increased the number of viable cells ($p < 0.05$) compared to parallel cultures of untreated cells (set to 100%), and these increases were maintained in cultures additionally treated with 10 μg/mL DJ callus extract and both 10 and 25 μg/mL DJ526 callus extract ($p < 0.05$). Further, cell viability did not fall below control (the baseline) in the presence of 100 μg/mL DJ or DJ526 extract, indicating no toxicity within the tested range. In addition, cell viability was not reduced by cotreatment with 200 μg/mL aspirin plus LPS compared to 1 μg/mL LPS alone and was still above baseline ($p < 0.05$). These findings indicate that extract concentrations of 10, 25, 50, and 100 μg/mL can be safely used for potential suppression of LPS-induced inflammatory activities in RAW264.7 cells.

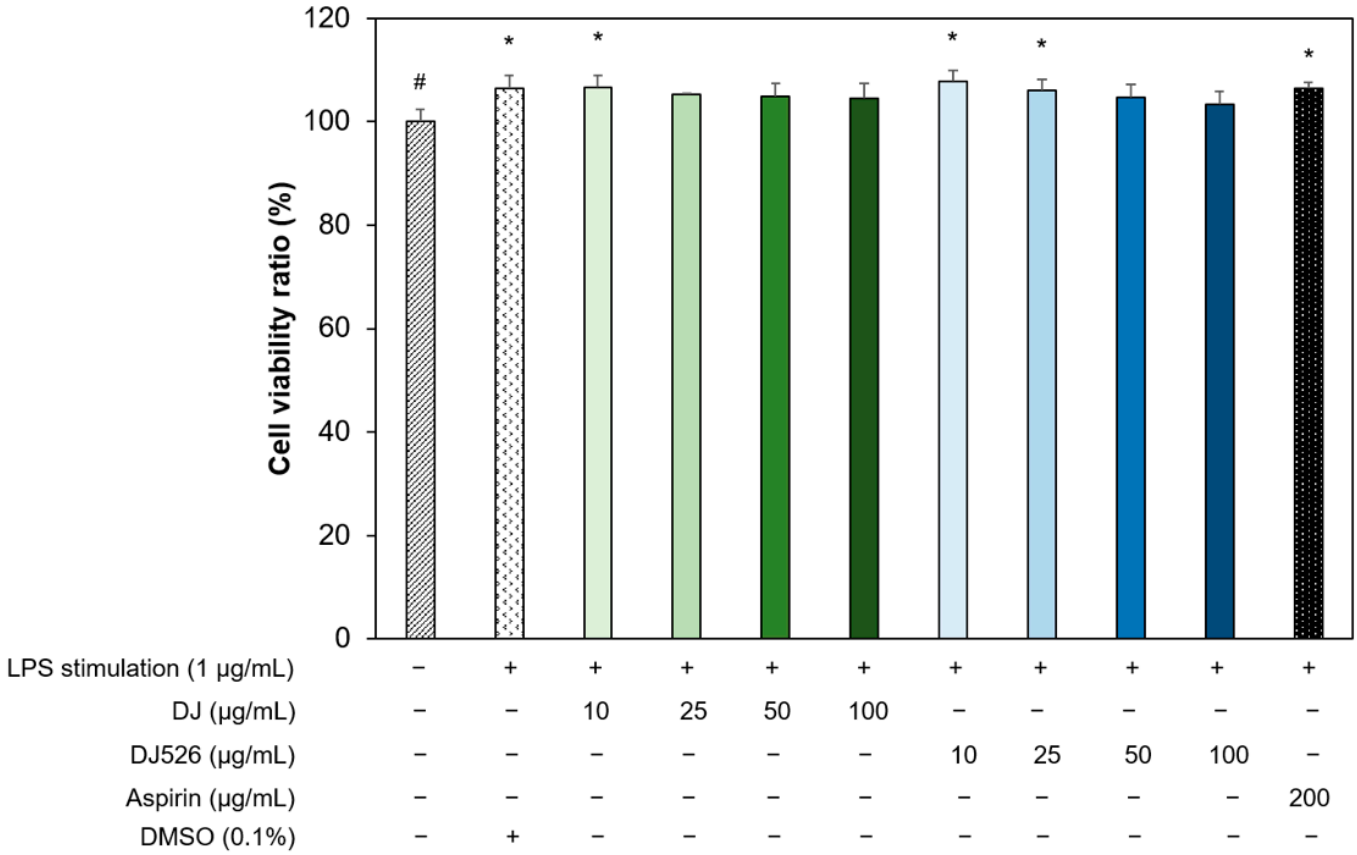

Figure 2. Low toxicities of DJ and DJ526 callus extracts. Concentrations up to 100 mg/mL had no effect on viable RAW264.7 cell numbers compared to untreated controls. The experiment was performed in triplicate (n = 3 for each replicate). Data are presented as mean ± standard deviation. * $p < 0.05$ vs. untreated controls; # $p < 0.05$ vs. cells treated with LPS alone.

3.3. Resveratrol-Enriched Rice Callus Extract Inhibited LPS-Induced NO Production by RAW264.7 Cells

Treatment of RAW264.7 cells with 1 μg/mL LPS markedly enhanced NO production (Figure 3), and this inflammatory response was substantially and dose-dependently reduced by resveratrol-enriched rice callus extract (DJ526) (all $p < 0.05$). In fact, the maximum inhibition at 100 μg/mL was comparable to that of 200 μg/mL aspirin (administered as a positive control). Moreover, this dose-dependent anti-inflammatory effect of DJ526 callus extract was markedly greater than that of DJ callus extract at all equivalent doses. These results strongly suggest that piceid and resveratrol enrichment contribute to the anti-inflammatory efficacy of rice callus extract.

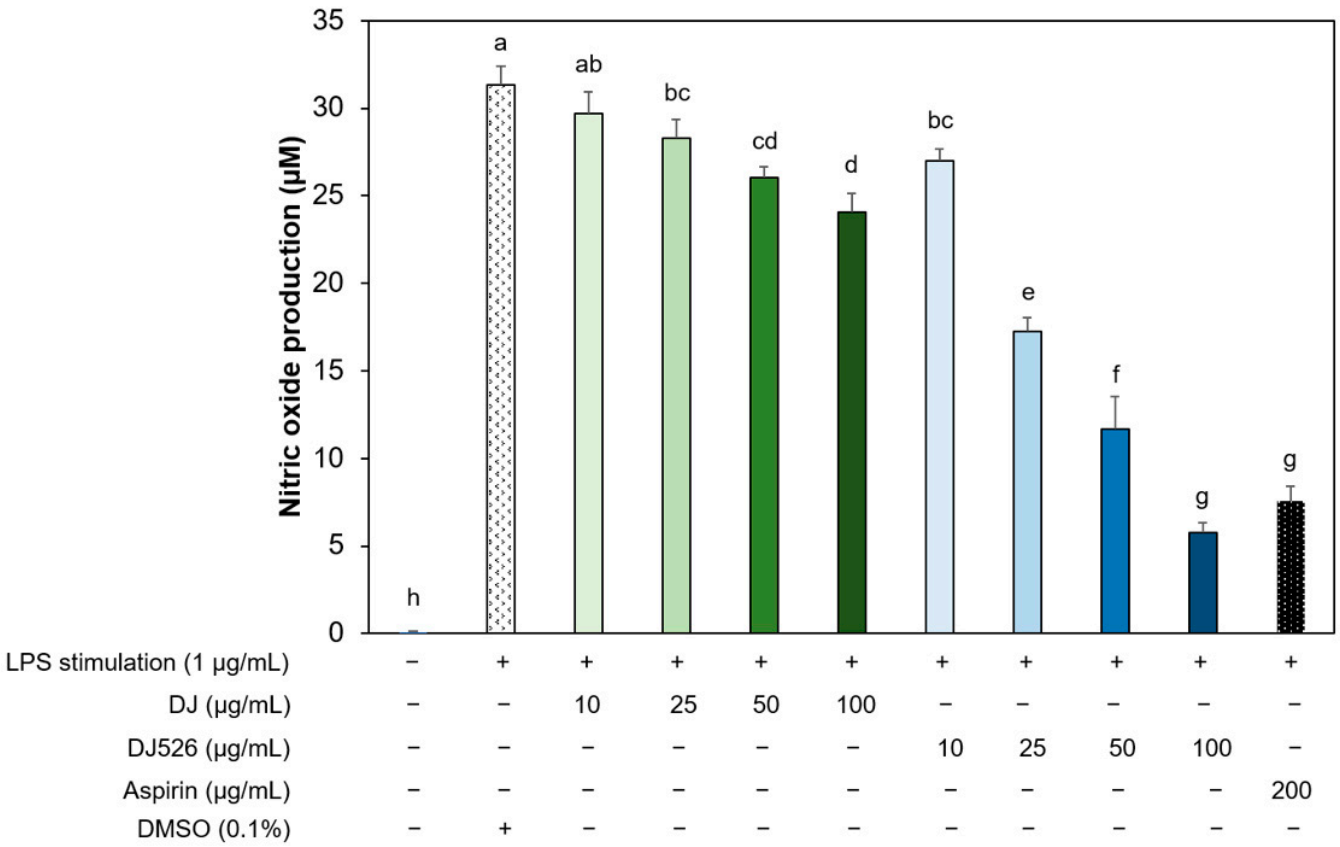

Figure 3. Suppression of LPS-induced NO production in RAW264.7 cells by DJ and DJ526 callus extracts. The experiment was performed in triplicate (n = 3 for each replicate). Data are presented as mean ± standard deviation. The increase in NO production induced by LPS was dose-dependently inhibited by DJ callus extract and more substantially by DJ526 callus extract enriched in resveratrol and piceid. The NO production by cells treated with LPS alone ("a") is the reference value for statistical comparison. Letters (a–h) indicate significant differences ($p < 0.05$) between treatments (where a > b > c > d > e > f > g > h).

3.4. Resveratrol-Enriched Rice Callus Extract Suppressed LPS-Induced Upregulation of Multiple Proinflammatory Genes in RAW264.7 Cells

Treatment with DJ rice callus extract also dose-dependently reduced LPS-induced upregulation of multiple proinflammatory genes (all $p < 0.05$), including the inflammatory mediator genes *iNOS* and *COX-2*, proinflammatory cytokine genes *IL-1β*, *IL-6*, and *TNF-α*, and the LPS receptor gene *TLR-4* compared to untreated controls (Figure 4). Consistent with effects on NO, DJ526 callus extract evoked markedly greater downregulation of these genes, including *iNOS*, at all concentrations compared to DJ callus extract ($p < 0.05$). Moreover, this anti-inflammatory effect was equivalent to or greater than that of aspirin. Thus, enrichment of resveratrol and piceid in rice callus extract substantially enhanced the suppression of LPS-induced inflammatory responses by RAW264.7 cells.

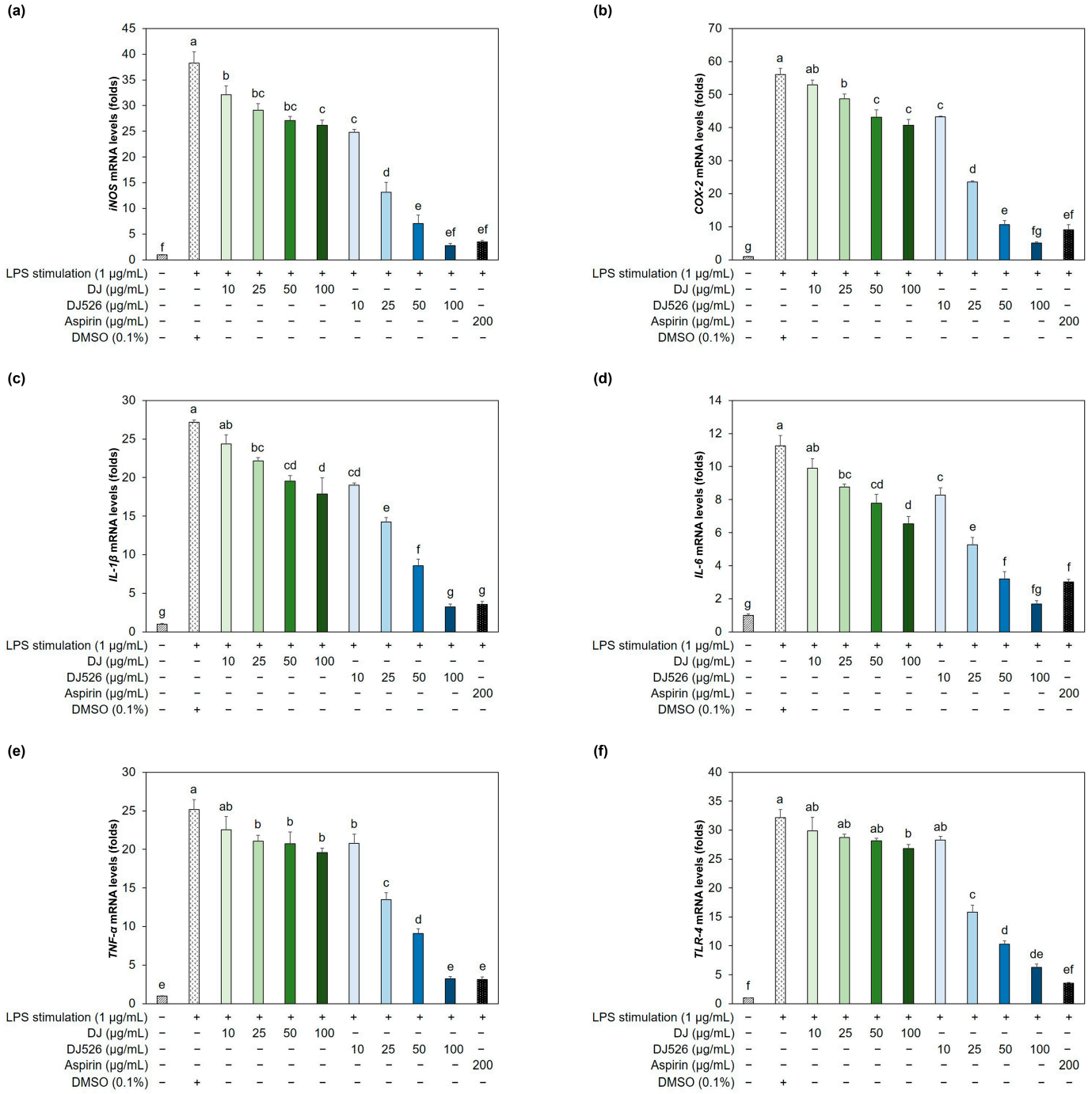

Figure 4. DJ and DJ526rice callus extract potently decreased the lipopolysaccharide-induced upregulation of proinflammatory genes in RAW264.7 cells. Pretreatment with DJ526 rice callus extract substantially reversed the LPS-evoked upregulation of (**a**) *iNOS*, (**b**) *COX-2*, (**c**) *IL-1β*, (**d**) *IL-6*, (**e**) *TNF-α*, and (**f**) *TLR-4*. The experiment was performed in triplicate ($n = 3$ for each replicate). Data are presented as mean ± standard deviation. The gene expression levels of LPS-treated cells ("a") are the reference values for statistical comparison. Letters (a–g) indicate significant differences ($p < 0.05$) between treatments (where a > b > c > d > e > f > g).

3.5. Resveratrol-Enriched Rice Callus Extract Reduced the Production of PGE_2 by LPS-Stimulated RAW264.7 Cells

Treatment with these extracts also significantly reduced LPS-evoked PGE_2 production ($p < 0.05$) in RAW264.7 cells (Figure 5), consistent with downregulation of *COX-2*, an enzyme required for PGE_2 synthesis. Again, the DJ526 callus extract was markedly more

potent than the DJ callus extract at equivalent concentrations, and the maximum effect was comparable to that of aspirin.

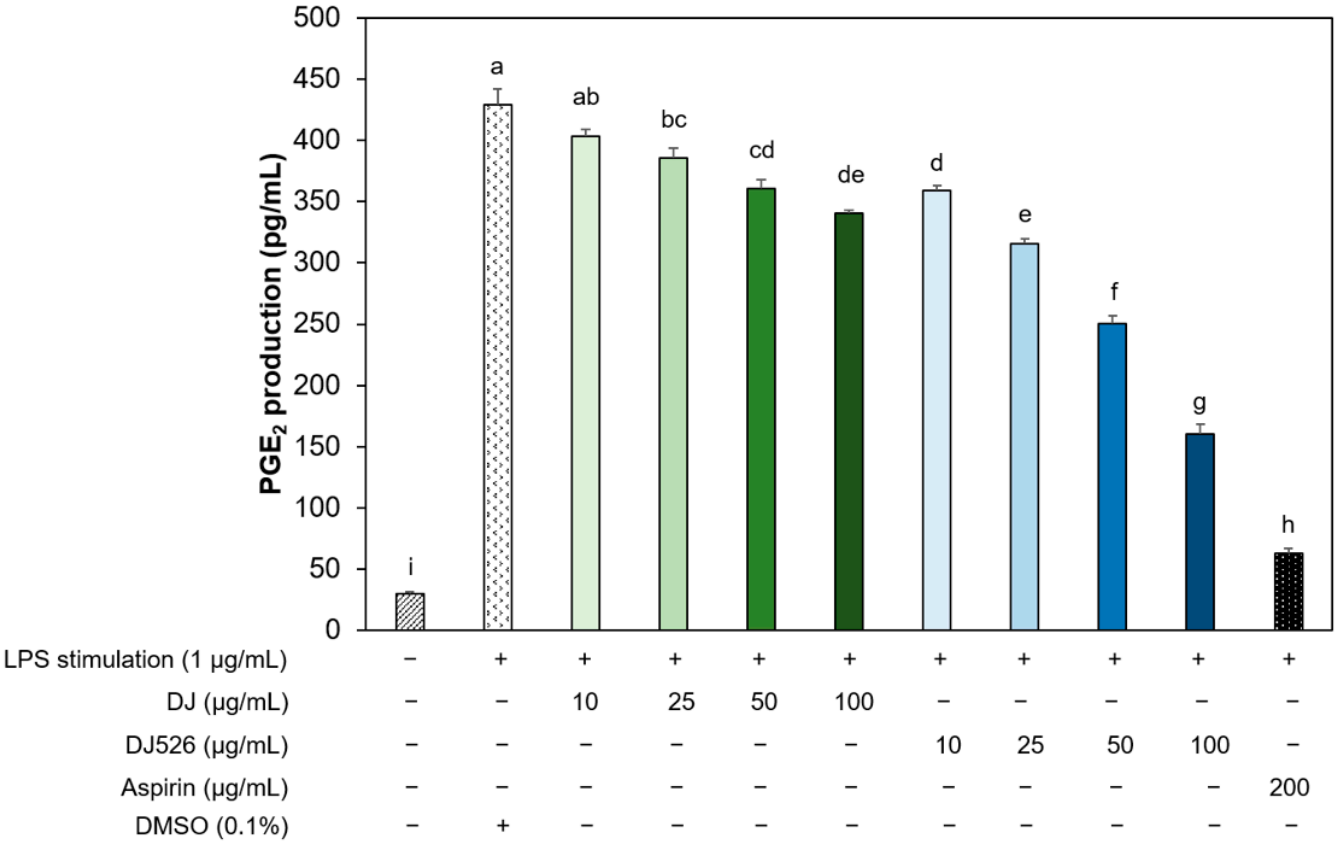

Figure 5. The DJ and DJ526 rice callus extracts dose-dependently inhibited LPS-induced PGE_2 production by RAW264.7 cells. The experiment was performed in triplicate (n = 2 for each replicate). Data are presented as mean ± standard deviation. The PGE_2 production by the LPS-treated cell group ("a") is the reference value for statistical comparison. Letters (a–i) indicate significant differences ($p < 0.05$) between the treatments (where a > b > c > d > e > f > g > h > i).

3.6. Resveratrol-Enriched Rice Callus Extract Inhibited MAPK and NF-κB Pathway Activation in LPS-Stimulated RAW264.7 Cells

Stimulation of RAW264.7 cells with LPS also activated inflammation-associated MAPK pathways, as evidenced by increased phosphorylation of MAPK isoforms ERK-1/2 (p-ERK-1/2) and p38 (p-p38) (Figure 6). Further, LPS stimulation also increased phosphorylation of the NF-κB active unit p65 (p-NF-κB p65). Consistent with downregulation of inflammation-associated genes (Figure 4), many of which are known targets of MAPK and NF-κB signaling, these phosphorylation events were dose-dependently reduced by DJ rice callus extract and more potently by DJ526 rice callus extract. Also consistent with downregulation of target genes, the maximum effect of DJ526 rice callus extract was comparable to that of aspirin. Indeed, 10–100 μg/mL DJ526 rice callus extract suppressed LPS-induced activation of MAPK and NF-κB signaling pathways and the downstream upregulation of multiple proinflammatory factors. Moreover, peak effects at the highest concentration (100 μg/mL) were comparable to those of aspirin and were not associated with any substantial reduction in cell viability (Figure 2), while the higher concentrations (125 and 150 μg/mL) caused a reduction in cell viability (Table S1).

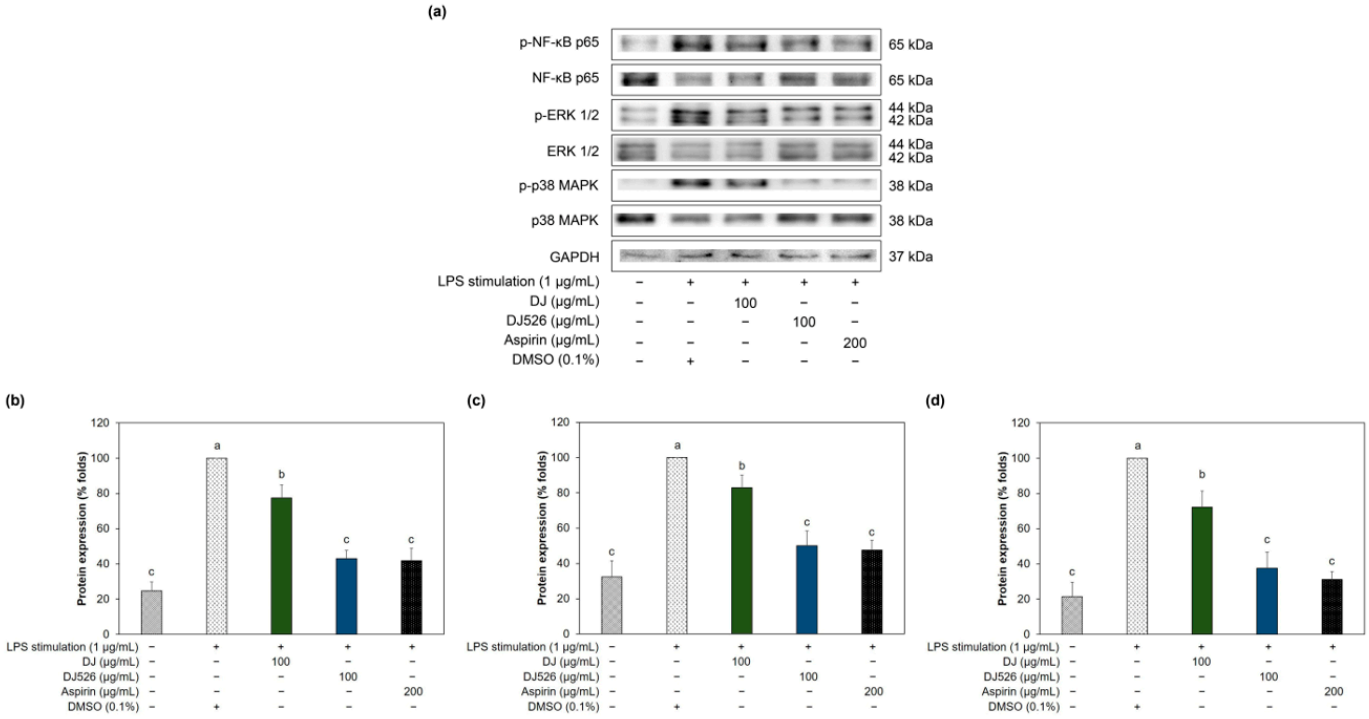

Figure 6. Both DJ and DJ526 rice callus extracts inhibited LPS-induced activation of MAPK and NF-κB signaling pathways in RAW264.7 cells. (**a**) Representative western blots. (**b**–**d**) Densitometric analyses of (**b**) p-NF-κB p65 protein expression, (**c**) p-ERK 1/2 protein expression, and (**d**) p-p38 protein expression. The experiment was performed in duplicate. Data are presented as mean ± standard deviation. Protein expression levels in cells treated with LPS alone ("a") are the reference values for statistical comparison. Letters (a–c) indicate significant differences ($p < 0.05$) between treatments (where a > b > c).

4. Discussion

Resveratrol exerts anti-inflammatory effects through several signaling pathways, such as NF-κB, MAPK, and the arachidonic acid pathway [39–41]. Arachidonic acid pathway inhibition plays a major role in the anti-inflammatory activity of resveratrol [41,42]. Resveratrol inhibits the activity of COX-1, leading to a reduction in prostaglandin production [43]. In PMA-treated human mammary epithelial cells, resveratrol directly inhibits the activity of COX-2, leading to the inhibition of PGE_2 production [44]. Therefore, resveratrol inhibits inflammatory responses through the arachidonic acid pathway by suppressing the activity of COX-1 and COX-2. The activation of NF-κB by LPS leads to the release of inflammatory mediators such as pro-inflammatory cytokines and NO [45]. Resveratrol decreased the expression of TLR-4 (the LPS-associated receptor), leading to the reduction of IL-6, iNOS, and NO by preventing the translocation of NF-κB p65 to the nucleus [46]. Resveratrol is able to suppress the inflammatory response by blocking the phosphorylation protein expression of p65 and IκB from the NF-κB signaling as well as phosphorylation of p38 and ERK from MAPK signaling under mastitis conditions [47].

Introduction of the resveratrol synthesis enzyme gene *STS* from peanut into the genome of Dongjin rice (creating the DJ526 line) markedly enhanced the concentrations of resveratrol and the resveratrol metabolite piceid in both seeds and calluses induced and expanded using 2N6 and 2MS-NO_3-free liquid media, respectively. Callus induction dramatically enhanced piceid content to 85.43 ± 3.44 μg/g dry weight from 4.72 ± 0.02 μg/g dry weight in DJ526 rice seeds or 17.10 ± 0.73-fold, and resveratrol content to 3.94 ± 0.02 μg/g dry weight from 2.605 ± 0.001 μg/g dry weight in DJ526 seeds or 1.52 ± 0.01-fold [32]. This enrichment markedly enhanced the anti-inflammatory activity of DJ526 callus extract compared to DJ callus extract. Thus, these DJ526-derived calluses are an excellent

source of anti-inflammatory resveratrol and piceid for the treatment or prevention of inflammatory diseases.

Based on the demonstrated anti-inflammatory efficacy of DJ526 rice seed extract enriched in resveratrol and piceid [32] and the further enrichment observed in the extract from callus, we predicted that the DJ526 callus extract would suppress LPS-induced inflammatory activity with high potency. Thus, DJ526 rice callus extract is essentially noncytotoxic within the effective anti-inflammatory range. Further, these anti-inflammatory effects were substantially greater than those of DJ extracts, suggesting that resveratrol and piceid enrichment augment the anti-inflammatory activity of endogenous rice phytochemicals.

Macrophages exhibit different phenotypes at different stages of the inflammatory response [48]. Macrophages have at least two different polarizations, the classical (M1) and alternative (M2) [49,50]. M1 and M2 macrophages can provide for their biological activities by secreting different cytokines and effector molecules [51]. The activation of M1 macrophages is associated with cytokine secretion for antigen defense, including antibacterial, anti-viral, and anti-tumor functions [52]. Treatment of DJ526 (without LPS) on macrophage cells significantly increased the expression of pro-inflammatory cytokines such as *COX-2*, *IL-1β*, *IL-6*, and *TNF-α* (Figure S4 and Table S2). The activation of M2 macrophages relates to the natural inflammation resolution. Therefore, M2 macrophages are usually mentioned as having repair or anti-inflammatory functions [53]. Numerous studies have reported that LPS activates the macrophage inflammatory response [54–56]. Lipopolysaccharide is recognized by TLR-4 and MD-2, which are abundantly expressed by macrophages and other innate immune cells [57–59], and stimulation of these receptors activates intracellular cascades such as MAPK and NF-κB signaling pathways. These activated pathways in turn upregulate the expression levels of enzymes that generate proinflammatory factors, such as iNOS, the enzyme generating NO, and COX-2, an enzyme producing prostaglandins such as PGE_2, as well as proinflammatory cytokines like IL-1β. All of these proinflammatory changes were dose-dependently suppressed by DJ526 rice callus extract and less potently by DJ rice callus extract. Moreover, the reductions evoked by DJ526 callus extract were significantly ($p = 0.01$) correlated with piceid and resveratrol contents according to Pearson's correlation analysis [*TLR-4* ($r = -0.92830$), *iNOS* ($r = -0.91994$), *COX-2* ($r = -0.91493$), *IL-1β* ($r = -0.94282$), *IL-6* ($r = -0.90036$), and *TNF-α* ($r = -0.96397$)] (Figure S5).

These results are consistent with the report by [60] that LPS activates macrophages via cell-surface TLR-4, leading to enhanced production and release of inflammatory cytokines such as TNF-α and IL-6, while resveratrol at 25 μM significantly downregulated the expression of TLR-4, TNF-α, and IL-6 at both mRNA and protein levels [60]. Zong et al. [61] also reported that 10 μM resveratrol significantly suppressed TNF-α, COX-2, IL-1β, and iNOS protein and mRNA expression levels, as well as the production of NO and PGE_2. Similarly, Bigagli et al. [62] reported that 5 and 10 μM resveratrol significantly reduced the production of NO and PGE_2 by LPS-stimulated RAW264.7 cells. Here, we show that a rich natural source of resveratrol (DJ526 rice callus) can suppress LPS-induced macrophage activation without inherent cytotoxicity. Moreover, the decreases in NO and PGE_2 production were again significantly ($p = 0.01$) correlated with the amount of piceid and resveratrol contained in DJ526 callus extract [$r = -0.94071$ for NO production (Figure S6) and $r = -0.97022$ for PGE_2 production (Figure S7)].

Both the NF-κB and MAPK pathways are activated during inflammation, as evidenced by the phosphorylation of critical pathway signaling proteins [63]. In turn, these pathways directly or indirectly activate proinflammatory genes [60,64–66], including *iNOS*, *TNF-α*, *IL-6*, *IL-1β*, and *COX-2* [67–70], that can facilitate the elimination of infectious pathogens and damaged cells [71,72]. The phosphorylation levels of proteins involved in the NF-κB and MAPK pathways were substantially reduced by resveratrol-enriched callus rice extract in LPS-stimulated RAW264.7 cells. The precise mechanisms for these effects warrant further study.

5. Conclusions

We demonstrate that piceid and resveratrol enriched in DJ526 rice seed are further enriched by callus induction and that callus extract can potently suppress the LPS-induced inflammatory activation of RAW264.7 macrophages. These anti-inflammatory effects included suppression of MAPK and NF-κB pathway activity and downregulation of *IL-1β*, *IL-6*, *TNF-α*, *TLR-4*, *COX-2*, *iNOS*, NO, and PGE_2 expression and/or release. We conclude that the piceid and resveratrol contents in DJ526 rice seed can be increased by callus induction and that callus extract is a potent and nontoxic anti-inflammatory.

Supplementary Materials: The following supporting information can be downloaded at: https://www.mdpi.com/article/10.3390/immuno4020009/s1. Figure S1: Sample chromatographs (left panel) and calibration standard curves for piceid (right upper panel) and resveratrol (right lower panel); Figure S2: The standard curve of sodium nitrite; Figure S3: Standard curve of PGE2 production; Figure S4: The expression levels of pro-inflammatory-associated genes in the RPMI-, DJ-, and DJ526-treated cells. Letters (a–c) indicate significant differences ($p < 0.05$) between treatments (where a > b > c); Figure S5: Pearson's correlation analyses between the amount of resveratrol (piceid + resveratrol) and mRNA levels; Figure S6: Pearson's correlation analyses between the amount of resveratrol (piceid + resveratrol) and nitric oxide production; Figure S7: Pearson's correlation analyses between the amount of resveratrol (piceid + resveratrol) and PGE2 production; Table S1: Cell viability assay results using the EZ-Cytox Cell Viability Assay Kit; Table S2: The mRNA levels of pro-inflammatory-associated cytokines.

Author Contributions: Conceptualization, S.-H.B.; methodology, C.M. and J.-S.K.; software, C.M.; validation, C.M., J.-S.K. and S.-H.B.; formal analysis, C.M.; investigation, C.M. and J.-S.K.; resources, S.-H.B.; data curation, C.M.; writing, original draft preparation, C.M.; writing, review, and editing, S.-H.B.; visualization, S.-H.B.; supervision, S.-H.B.; project administration, S.-H.B.; funding acquisition, S.-H.B. All authors have read and agreed to the published version of the manuscript.

Funding: This research was supported by the Sunchon National University Research Fund (Grant number: 2023-0310).

Institutional Review Board Statement: Not applicable.

Informed Consent Statement: Not applicable.

Data Availability Statement: All data generated for this project are included in the manuscript. The authors will provide additional details upon reasonable request.

Conflicts of Interest: The authors declare no conflicts of interest.

References

1. Zhao, H.; Wu, L.; Yan, G.; Chen, Y.; Zhou, M.; Wu, Y.; Li, Y. Inflammation and tumor progression: Signaling pathways and targeted intervention. *Signal Transduct. Target. Ther.* **2021**, *6*, 263. [CrossRef] [PubMed]
2. Medzhitov, R. Origin and physiological roles of inflammation. *Nature* **2008**, *454*, 428–435. [CrossRef] [PubMed]
3. Wang, J.; Wang, H.; Zhang, H.; Liu, Z.; Ma, C.; Kang, W. Immunomodulation of ADPs-1a and ADPs-3a on RAW264.7 cells through NF-κB/MAPK signaling pathway. *Int. J. Biol. Macromol.* **2019**, *132*, 1024–1030. [CrossRef] [PubMed]
4. Liu, X.; Yin, S.; Chen, Y.; Wu, Y.; Zheng, W.; Dong, H.; Bai, Y.; Qin, Y.; Li, J.; Feng, S.; et al. LPS-induced proinflammatory cytokine expression in human airway epithelial cells and macrophages via NF-κB, STAT3 or AP-1 activation. *Mol. Med. Rep.* **2018**, *17*, 5484–5491. [CrossRef] [PubMed]
5. Han, S.; Chen, Z.; Han, P.; Hu, Q.; Xiao, Y. Activation of macrophages by lipopolysaccharide for assessing the immunomodulatory property of biomaterials. *Tissue Eng. Part. A* **2017**, *23*, 1100–1109. [CrossRef] [PubMed]
6. Hou, W.; Hu, S.; Su, Z.; Wang, Q.; Meng, G.; Guo, T.; Zhang, J.; Gao, P. Myricetin attenuates LPS-induced inflammation in RAW 264.7 macrophages and mouse models. *bioRxiv* **2018**, 299420. [CrossRef] [PubMed]
7. Ngkelo, A.; Meja, K.; Yeadon, M.; Adcock, I.; Kirkham, P.A. LPS induced inflammatory responses in human peripheral blood mononuclear cells is mediated through NOX_4 and Giα dependent PI-3kinase signalling. *J. Inflamm.* **2012**, *9*, 1. [CrossRef] [PubMed]
8. Raduolovic, K.; Mak'Anyengo, R.; Kaya, B.; Steinert, A.; Niess, J.H. Injections of lipopolysaccharide into mice to mimic entrance of microbial-derived products after intestinal barrier breach. *J. Vis. Exp.* **2018**, *135*, e57610. [CrossRef]

9. Tucureanu, M.M.; Rebleanu, D.; Constantinescu, C.A.; Deleanu, M.; Voicu, G.; Butoi, E.; Calin, M.; Manduteanu, I. Lipopolysaccharide-induced inflammation in monocytes/macrophages is blocked by liposomal delivery of G(i)-protein inhibitor. *Int. J. Nanomed.* **2018**, *13*, 63–76. [CrossRef] [PubMed]
10. Lull, C.; Wichers, H.J.; Savelkoul, H.F.J. Antiinflammatory and immunomodulating properties of fungal metabolites. *Mediat. Inflamm.* **2005**, *2005*, 892572. [CrossRef] [PubMed]
11. Zhao, Y.; Liu, X.; Qu, Y.; Wang, L.; Geng, D.; Chen, W.; Li, L.; Tian, Y.; Chang, S.; Zhao, C.; et al. The roles of p38 MAPK → COX_2 and NF-κB → COX_2 signal pathways in age-related testosterone reduction. *Sci. Rep.* **2019**, *9*, 10556. [CrossRef] [PubMed]
12. Park, H.H.; Kim, M.J.; Li, Y.; Park, Y.N.; Lee, J.; Lee, Y.J.; Kim, S.G.; Park, H.J.; Son, J.K.; Chang, H.W.; et al. Britanin suppresses LPS-induced nitric oxide, PGE_2 and cytokine production via NF-κB and MAPK inactivation in RAW 264.7 cells. *Int. Immunopharmacol.* **2013**, *15*, 296–302. [CrossRef] [PubMed]
13. Athar, M.; Back, J.H.; Tang, X.; Kim, K.H.; Kopelovich, L.; Bickers, D.R.; Kim, A.L. Resveratrol: A review of preclinical studies for human cancer prevention. *Toxicol. Appl. Pharmacol.* **2007**, *224*, 274–283. [CrossRef] [PubMed]
14. Szajdek, A.; Borowska, E.J. Bioactive compounds and health-promoting properties of berry fruits: A review. *Plant Foods Hum. Nutr.* **2008**, *63*, 147–156. [CrossRef] [PubMed]
15. Arya, S.S.; Salve, A.R.; Chauhan, S. Peanuts as functional food: A review. *J. Food Sci. Technol.* **2016**, *53*, 31–41. [CrossRef] [PubMed]
16. Sebastià, N.; Montoro, A.; Mañes, J.; Soriano, J.M. A preliminary study of presence of resveratrol in skins and pulps of European and Japanese plum cultivars. *J. Sci. Food Agric.* **2012**, *92*, 3091–3094. [CrossRef] [PubMed]
17. Banez, M.J.; Geluz, M.I.; Chandra, A.; Hamdan, T.; Biswas, O.S.; Bryan, N.S.; Von Schwarz, E.R. A systemic review on the antioxidant and anti-inflammatory effects of resveratrol, curcumin, and dietary nitric oxide supplementation on human cardiovascular health. *Nutr. Res.* **2020**, *78*, 11–26. [CrossRef]
18. Sharifi-Rad, J.; Quispe, C.; Durazzo, A.; Lucarini, M.; Souto, E.B.; Santini, A.; Imran, M.; Moussa, A.Y.; Mostafa, N.M.; El-Shazly, M.; et al. Resveratrol' biotechnological applications: Enlightening its antimicrobial and antioxidant properties. *J. Herb. Med.* **2022**, *32*, 100550. [CrossRef]
19. Vestergaard, M.; Ingmer, H. Antibacterial and antifungal properties of resveratrol. *Int. J. Antimicrob. Agents* **2019**, *53*, 716–723. [CrossRef] [PubMed]
20. Ferraz da Costa, D.C.; Pereira Rangel, L.; Martins-Dinis, M.M.; Ferretti, G.D.; Ferreira, V.F.; Silva, J.L. Anticancer potential of resveratrol, β-lapachone and their analogues. *Molecules* **2020**, *25*, 893. [CrossRef] [PubMed]
21. Angellotti, G.; Di Prima, G.; Belfiore, E.; Campisi, G.; De Caro, V. Chemopreventive and anticancer role of resveratrol against oral squamous cell carcinoma. *Pharmaceutics* **2023**, *15*, 275. [CrossRef] [PubMed]
22. Meng, T.; Xiao, D.; Muhammed, A.; Deng, J.; Chen, L.; He, J. Anti-inflammatory action and mechanisms of resveratrol. *Molecules* **2021**, *26*, 229. [CrossRef] [PubMed]
23. Chen, L.Z.; Yao, L.; Jiao, M.M.; Shi, J.B.; Tan, Y.; Ruan, B.F.; Liu, X.H. Novel resveratrol-based flavonol derivatives: Synthesis and anti-inflammatory activity in vitro and in vivo. *Eur. J. Med. Chem.* **2019**, *175*, 114–128. [CrossRef] [PubMed]
24. Hsu, Y.-A.; Chen, C.-S.; Wang, Y.-C.; Lin, E.-S.; Chang, C.-Y.; Chen, J.J.; Wu, M.-Y.; Lin, H.-J.; Wan, L. Anti-inflammatory effects of resveratrol on human retinal pigment cells and a myopia animal model. *Curr. Issues Mol. Biol.* **2021**, *43*, 716–727. [CrossRef] [PubMed]
25. Griñán-Ferré, C.; Bellver-Sanchis, A.; Izquierdo, V.; Corpas, R.; Roig-Soriano, J.; Chillón, M.; Andres-Lacueva, C.; Somogyvári, M.; Sőti, C.; Sanfeliu, C.; et al. The pleiotropic neuroprotective effects of resveratrol in cognitive decline and Alzheimer's disease pathology: From antioxidant to epigenetic therapy. *Ageing Res. Rev.* **2021**, *67*, 101271. [CrossRef] [PubMed]
26. Sawda, C.; Moussa, C.; Turner, R.S. Resveratrol for Alzheimer's disease. *Ann. N. Y. Acad. Sci.* **2017**, *1403*, 142–149. [CrossRef] [PubMed]
27. Arbo, B.D.; André-Miral, C.; Nasre-Nasser, R.G.; Schimith, L.E.; Santos, M.G.; Costa-Silva, D.; Muccillo-Baisch, A.L.; Hort, M.A. Resveratrol derivatives as potential treatments for Alzheimer's and Parkinson's disease. *Front. Aging Neurosci.* **2020**, *12*, 103. [CrossRef] [PubMed]
28. Zhong, L.-M.; Zong, Y.; Sun, L.; Guo, J.-Z.; Zhang, W.; He, Y.; Song, R.; Wang, W.-M.; Xiao, C.-J.; Lu, D. Resveratrol Inhibits Inflammatory Responses via the Mammalian Target of Rapamycin Signaling Pathway in Cultured LPS-Stimulated Microglial Cells. *PLoS ONE* **2012**, *7*, e32195. [CrossRef]
29. Pinheiro, D.M.L.; de Oliveira, A.H.S.; Coutinho, L.G.; Fontes, F.L.; de Medeiros Oliveira, R.K.; Oliveira, T.T.; Faustino, A.L.F.; Lira da Silva, V.; de Melo Campos, J.T.A.; Lajus, T.B.P.; et al. Resveratrol decreases the expression of genes involved in inflammation through transcriptional regulation. *Free Radic. Biol. Med.* **2019**, *130*, 8–22. [CrossRef] [PubMed]
30. Palomera-Ávalos, V.; Griñán-Ferré, C.; Izquierdo, V.; Camins, A.; Sanfeliu, C.; Canudas, A.M.; Pallàs, M. Resveratrol modulates response against acute inflammatory stimuli in aged mouse brain. *Exp. Gerontol.* **2018**, *102*, 3–11. [CrossRef] [PubMed]
31. Baek, S.-H.; Shin, W.-C.; Ryu, H.-S.; Lee, D.-W.; Moon, E.; Seo, C.-S.; Hwang, E.; Lee, H.-S.; Ahn, M.-H.; Jeon, Y.; et al. Creation of resveratrol-enriched rice for the treatment of metabolic syndrome and related diseases. *PLoS ONE* **2013**, *8*, e57930. [CrossRef] [PubMed]
32. Monmai, C.; Kim, J.-S.; Baek, S.-H. Use of germination to enhance resveratrol content and its anti-inflammatory activity in lipopolysaccharide-stimulated RAW264.7 cells. *Molecules* **2023**, *28*, 4898. [CrossRef] [PubMed]
33. Cho, D.-H.; Lim, S.-T. Changes in phenolic acid composition and associated enzyme activity in shoot and kernel fractions of brown rice during germination. *Food Chem.* **2018**, *256*, 163–170. [CrossRef] [PubMed]

34. Khan, M.; Park, S.; Kim, H.-J.; Lee, K.-J.; Kim, D.H.; Baek, S.-H.; Hong, S.-T. The resveratrol rice DJ526 callus significantly increases the lifespan of *Drosophila* (resveratrol rice DJ526 callus for longevity). *Nutrients* **2019**, *11*, 983. [CrossRef] [PubMed]
35. Monmai, C.; Kim, J.-S.; Baek, S.-H. Transgenic rice seed extracts exert immunomodulatory effects by modulating immune-related biomarkers in RAW264.7 macrophage cells. *Nutrients* **2022**, *14*, 4143. [CrossRef] [PubMed]
36. Kantayos, V.; Shin, W.-C.; Kim, J.-S.; Jeon, S.-H.; Rha, E.-S.; Baek, S.-H. Resveratrol-enriched rice identical to original Dongjin rice variety with respect to major agronomic traits in different cultivation years and regions. *GM Crops Food* **2021**, *12*, 449–458. [CrossRef]
37. Liu, Y.; Fang, S.; Li, X.; Feng, J.; Du, J.; Guo, L.; Su, Y.; Zhou, J.; Ding, G.; Bai, Y.; et al. Aspirin inhibits LPS-induced macrophage activation via the NF-κB pathway. *Sci. Rep.* **2017**, *7*, 11549. [CrossRef] [PubMed]
38. Wang, Q.; Liu, W.; Yue, Y.; Sun, C.; Zhang, Q. Proteoglycan from *Bacillus* sp. BS11 inhibits the inflammatory response by suppressing the MAPK and NF-κB pathways in lipopolysaccharide-induced RAW264.7 macrophages. *Mar. Drugs* **2020**, *18*, 585. [CrossRef] [PubMed]
39. Adhami, V.M.; Afaq, F.; Ahmad, N. Suppression of ultraviolet B exposure-mediated activation of NF-κB in normal human keratinocytes by resveratrol. *Neoplasia* **2003**, *5*, 74–82. [CrossRef] [PubMed]
40. Pirola, L.; Fröjdö, S. Resveratrol: One molecule, many targets. *IUBMB Life* **2008**, *60*, 323–332. [CrossRef] [PubMed]
41. Li, X.; Li, F.; Wang, F.; Li, J.; Lin, C.; Du, J. Resveratrol inhibits the proliferation of A549 cells by inhibiting the expression of COX-2. *OncoTargets Ther.* **2018**, *11*, 2981–2989. [CrossRef]
42. Magrone, T.; Magrone, M.; Russo, M.A.; Jirillo, E. Recent advances on the anti-Inflammatory and antioxidant properties of red grape polyphenols: In vitro and in vivo studies. *Antioxidants* **2020**, *9*, 35. [CrossRef]
43. Jang, M.; Cai, L.; Udeani, G.O.; Slowing, K.V.; Thomas, C.F.; Beecher, C.W.W.; Fong, H.H.S.; Farnsworth, N.R.; Kinghorn, A.D.; Mehta, R.G.; et al. Cancer chemopreventive activity of resveratrol, a natural product derived from grapes. *Science* **1997**, *275*, 218–220. [CrossRef] [PubMed]
44. Subbaramaiah, K.; Chung, W.J.; Michaluart, P.; Telang, N.; Tanabe, T.; Inoue, H.; Jang, M.; Pezzuto, J.M.; Dannenberg, A.J. Resveratrol inhibits cyclooxygenase-2 transcription and activity in phorbol ester-treated human mammary epithelial cells. *J. Biol. Chem.* **1998**, *273*, 21875–21882. [CrossRef] [PubMed]
45. Wang, T.; Wu, F.; Jin, Z.; Zhai, Z.; Wang, Y.; Tu, B.; Yan, W.; Tang, T. Plumbagin inhibits LPS-induced inflammation through the inactivation of the nuclear factor-kappa B and mitogen activated protein kinase signaling pathways in RAW 264.7 cells. *Food Chem. Toxicol.* **2014**, *64*, 177–183. [CrossRef] [PubMed]
46. Ma, C.; Wang, Y.; Dong, L.; Li, M.; Cai, W. Anti-inflammatory effect of resveratrol through the suppression of NF-κB and JAK/STAT signaling pathways. *Acta Biochim. Biophys. Sin.* **2015**, *47*, 207–213. [CrossRef] [PubMed]
47. Zhang, X.; Wang, Y.; Xiao, C.; Wei, Z.; Wang, J.; Yang, Z.; Fu, Y. Resveratrol inhibits LPS-induced mice mastitis through attenuating the MAPK and NF-κB signaling pathway. *Microb. Pathog.* **2017**, *107*, 462–467. [CrossRef] [PubMed]
48. Martinez, F.O.; Sica, A.; Mantovani, A.; Locati, M. Macrophage activation and polarization. *Front. Biosci.* **2008**, *13*, 453–461. [CrossRef] [PubMed]
49. Xue, J.; Schmidt, S.V.; Sander, J.; Draffehn, A.; Krebs, W.; Quester, I.; De Nardo, D.; Gohel, T.D.; Emde, M.; Schmidleithner, L.; et al. Transcriptome-based network analysis reveals a spectrum model of human macrophage activation. *Immunity* **2014**, *40*, 274–288. [CrossRef] [PubMed]
50. Mantovani, A.; Sozzani, S.; Locati, M.; Allavena, P.; Sica, A. Macrophage polarization: Tumor-associated macrophages as a paradigm for polarized M2 mononuclear phagocytes. *Trends Immunol.* **2002**, *23*, 549–555. [CrossRef] [PubMed]
51. Lv, R.; Bao, Q.; Li, Y. Regulation of M1-type and M2-type macrophage polarization in RAW264.7 cells by Galectin-9. *Mol. Med. Rep.* **2017**, *16*, 9111–9119. [CrossRef]
52. Lee, J.H.; Moon, S.H.; Kim, H.S.; Park, E.; Ahn, D.U.; Paik, H.D. Immune-enhancing activity of phosvitin by stimulating the production of pro-inflammatory mediator. *Poult. Sci.* **2017**, *96*, 3872–3878. [CrossRef] [PubMed]
53. Jablonski, K.A.; Amici, S.A.; Webb, L.M.; Ruiz-Rosado Jde, D.; Popovich, P.G.; Partida-Sanchez, S.; Guerau-de-Arellano, M. Novel markers to delineate murine M1 and M2 macrophages. *PLoS ONE* **2015**, *10*, e0145342. [CrossRef] [PubMed]
54. Tang, J.; Diao, P.; Shu, X.; Li, L.; Xiong, L. Quercetin and quercitrin attenuates the inflammatory response and oxidative stress in LPS-induced RAW264.7 cells: In vitro assessment and a theoretical model. *Biomed. Res. Int.* **2019**, *2019*, 7039802. [CrossRef] [PubMed]
55. Page, M.J.; Kell, D.B.; Pretorius, E. The role of lipopolysaccharide-induced cell signalling in chronic inflammation. *Chronic Stress.* **2022**, *6*, 24705470221076390. [CrossRef] [PubMed]
56. Cao, Y.; Chen, J.; Ren, G.; Zhang, Y.; Tan, X.; Yang, L. Punicalagin prevents inflammation in LPS-induced RAW264.7 macrophages by inhibiting FoxO3a/autophagy signaling pathway. *Nutrients* **2019**, *11*, 2794. [CrossRef] [PubMed]
57. Maeshima, N.; Fernandez, R. Recognition of lipid A variants by the TLR4-MD-2 receptor complex. *Front. Cell Infect. Microbiol.* **2013**, *3*, 3. [CrossRef] [PubMed]
58. Zamyatina, A.; Heine, H. Lipopolysaccharide recognition in the crossroads of TLR4 and Caspase-4/11 mediated inflammatory pathways. *Front. immunol* **2020**, *11*, 585146. [CrossRef] [PubMed]
59. Nijland, R.; Hofland, T.; van Strijp, J.A. Recognition of LPS by TLR4: Potential for anti-inflammatory therapies. *Mar. Drugs* **2014**, *12*, 4260–4273. [CrossRef] [PubMed]

60. Eo, H.J.; Kwon, H.Y.; Da Kim, S.; Kang, Y.; Park, Y.; Park, G.H. GC/MS analysis and anti-inflammatory effect of leaf extracts from *Hibiscus syriacus* through inhibition of NF-κB and MAPKs signaling in LPS-stimulated RAW264.7 macrophages. *Plant Biotechnol. Rep.* **2020**, *14*, 539–546. [CrossRef]
61. Zong, Y.; Sun, L.; Liu, B.; Deng, Y.S.; Zhan, D.; Chen, Y.L.; He, Y.; Liu, J.; Zhang, Z.J.; Sun, J.; et al. Resveratrol inhibits LPS-induced MAPKs activation via activation of the phosphatidylinositol 3-kinase pathway in murine RAW 264.7 macrophage cells. *PLoS ONE* **2012**, *7*, e44107. [CrossRef] [PubMed]
62. Bigagli, E.; Cinci, L.; Paccosi, S.; Parenti, A.; D'Ambrosio, M.; Luceri, C. Nutritionally relevant concentrations of resveratrol and hydroxytyrosol mitigate oxidative burst of human granulocytes and monocytes and the production of pro-inflammatory mediators in LPS-stimulated RAW 264.7 macrophages. *Int. Immunopharmacol.* **2017**, *43*, 147–155. [CrossRef] [PubMed]
63. Ren, J.; Su, D.; Li, L.; Cai, H.; Zhang, M.; Zhai, J.; Li, M.; Wu, X.; Hu, K. Anti-inflammatory effects of Aureusidin in LPS-stimulated RAW264.7 macrophages via suppressing NF-κB and activating ROS- and MAPKs-dependent Nrf2/HO-1 signaling pathways. *Toxicol. Appl. Pharmacol.* **2020**, *387*, 114846. [CrossRef] [PubMed]
64. Jin, W.; Jia, Y.; Huang, L.; Wang, T.; Wang, H.; Dong, Y.; Zhang, H.; Fan, M.; Lv, P. Lipoxin A4 methyl ester ameliorates cognitive deficits induced by chronic cerebral hypoperfusion through activating ERK/Nrf2 signaling pathway in rats. *Pharmacol. Biochem. Behav.* **2014**, *124*, 145–152. [CrossRef] [PubMed]
65. Tong, W.; Chen, X.; Song, X.; Chen, Y.; Jia, R.; Zou, Y.; Li, L.; Yin, L.; He, C.; Liang, X.; et al. Resveratrol inhibits LPS-induced inflammation through suppressing the signaling cascades of TLR4-NF-κB/MAPKs/IRF3. *Exp. Ther. Med.* **2020**, *19*, 1824–1834. [CrossRef] [PubMed]
66. Kim, M.G.; Kim, S.; Boo, K.-H.; Kim, J.-H.; Kim, C.S. Anti-inflammatory effects of immature *Citrus unshiu* fruit extracts via suppression of NF-κB and MAPK signal pathways in LPS-induced RAW264.7 macrophage cells. *Food Sci. Biotechnol.* **2023**, *33*, 903–911. [CrossRef] [PubMed]
67. Chen, Y.; Ji, N.; Pan, S.; Zhang, Z.; Wang, R.; Qiu, Y.; Jin, M.; Kong, D. Roburic acid suppresses NO and IL-6 production via targeting NF-κB and MAPK pathway in RAW264.7 cells. *Inflammation* **2017**, *40*, 1959–1966. [CrossRef] [PubMed]
68. Yu, X.; Zhang, F.; Shi, J. Effect of sevoflurane treatment on microglia activation, NF-kB and MAPK activities. *Immunobiology* **2019**, *224*, 638–644. [CrossRef] [PubMed]
69. Frattaruolo, L.; Carullo, G.; Brindisi, M.; Mazzotta, S.; Bellissimo, L.; Rago, V.; Curcio, R.; Dolce, V.; Aiello, F.; Cappello, A.R. Antioxidant and anti-inflammatory activities of flavanones from *Glycyrrhiza glabra* L. (licorice) leaf phytocomplexes: Identification of licoflavanone as a modulator of NF-kB/MAPK pathway. *Antioxidants* **2019**, *8*, 186. [CrossRef] [PubMed]
70. Gao, H.; Kang, N.; Hu, C.; Zhang, Z.; Xu, Q.; Liu, Y.; Yang, S. Ginsenoside Rb1 exerts anti-inflammatory effects in vitro and in vivo by modulating toll-like receptor 4 dimerization and NF-kB/MAPKs signaling pathways. *Phytomedicine* **2020**, *69*, 153197. [CrossRef] [PubMed]
71. Yu, H.; Lin, L.; Zhang, Z.; Zhang, H.; Hu, H. Targeting NF-κB pathway for the therapy of diseases: Mechanism and clinical study. *Signal Transduct. Target. Ther.* **2020**, *5*, 209. [CrossRef] [PubMed]
72. Guo, Z.; Kang, S.; Wu, Q.; Wang, S.; Crickmore, N.; Zhou, X.; Bravo, A.; Soberón, M.; Zhang, Y. The regulation landscape of MAPK signaling cascade for thwarting Bacillus thuringiensis infection in an insect host. *PLoS Pathog.* **2021**, *17*, e1009917. [CrossRef] [PubMed]